



# Modeling and estimation of thrust force, torque, and surface roughness in indexable drilling of AA6061-T651 with Taguchi, ANN, and ANFIS

ASLAN AKDULUM\*<sup>ID</sup> and YUNUS KAYIR<sup>ID</sup>

Department of Manufacturing Engineering, Faculty of Technology, Gazi University, Ankara, Turkey  
e-mail: a.akdulum@gmail.com; ykayir@gazi.edu.tr

MS received 16 December 2022; revised 2 June 2023; accepted 8 June 2023

**Abstract.** In this study, the effect of drilling 6061-T651 aluminum alloy with different lengths of indexable insert drills, called U drills, on thrust force, torque, and surface roughness was investigated. As input parameters, length-to-diameter ratio, feed rate, and cutting speed were chosen for experimental works. The optimum values of the test parameters were determined by the ratio of signal to noise. In addition, output responses were modeled and compared with Taguchi, artificial neural networks (ANN), and the adaptive neuro-fuzzy inference system (ANFIS) methods. Both the experimental results and the signal-to-noise ratios derived from the experimental results were employed in the modeling process. The models with the highest accuracy were created using ANN when the predicted results from the models were compared to the experimental findings. The MAPE values of the ANN model created with the SN ratio were obtained as 0.18% for thrust force, 0.17% for torque, and 1.79% for surface roughness. Converting the output responses to SN ratios and using them in the models enabled the estimation of thrust, torque, and surface roughness with less error and satisfactory reliability. With the method proposed in this study, output responses according to input variables can be predicted with higher precision, resulting in the efficiency and reliability required by the industry.

**Keywords.** 6061-T651; U drill; ANN; ANFIS; taguchi; prediction.

## 1. Introduction

6061-T651 is an aluminum alloy containing more magnesium and silicon than other elements [1]. These high-alloying elements contribute to the increase in strength of the material by forming Mg and Si-based precipitates with the precipitation hardening process [2]. The prominent mechanical characteristics of this alloy, such as its high strength, superior weldability, and light weight, are the primary factors in its selection [3]. It is widely used in industries such as advanced structural components, automobiles, storage tanks, frames, high-speed trains, pipelines, shipbuilding, and defense, especially in the aircraft and aerospace industry [2, 4]. The rate of hole drilling among the total metal cutting operations is estimated to be 36% when all machines are taken into account and 40% when CNC machines are taken into account [5]. Drilling operations have an important place in the sectors where this material is used. Due to the semi-enclosed environment in which drilling is performed, there are issues including friction between the cutting tool and the workpiece, high drilling temperatures, and challenges with chip removal [6].

In the processing of aluminum materials, phenomena such as friction, adhesion, and chip evacuation can adversely affect the drilling process and hole quality [7]. It is crucial to establish the ideal input parameter values in order to solve such difficulties. The key influencing elements for output reactions such thrust force, torque, and surface roughness in machining operations are feed rate and cutting speed [8]. In addition to these variables, the cutting tool is vital to the operation's optimization. It is estimated that the largest amount of money in the cutting tool class is spent on drills [9]. In the drilling tool market, U drills are estimated to have a 53% market share [10]. Although it has a high market share, there are not enough scientific studies about the U drill. Drilling of aluminum alloys with the U drill is very limited and quite insufficient [11–14]. When the literature was scanned, no study was found in which 6061 aluminum alloy was drilled with a U drill. The fact that there is so little research on it causes the cutting tool to not be used efficiently and causes unnecessary cost increases for the industry. Proper selection of drilling parameters contributes to increased hole quality, optimum drilling forces, and a more efficient drilling process [5]. In the highly competitive industry, choosing and knowing the optimum drilling parameters is very important for quality

\*For correspondence  
Published online: 19 July 2023

[15]. Because, in a competitive environment, it has a direct and significant impact on cost [16]. In drilling, feed rate, cutting speed, and cutter type directly affect the drilling time. One of the most significant cost indicators is time. Scientific studies in the academic field will guide the determination of the optimum processing parameters needed by the industry, thus obtaining the desired output responses at the optimum cost [17]. Various algorithms and artificial intelligence techniques, such as fuzzy logic and artificial neural networks, as well as experimental, analytical, mathematical, and numerical approaches are used to explore the determination of the best processing parameters and how they affect output responses [18]. 6061 aluminum alloy has been studied in various studies on hole drilling. Chern and Lee [19] experimentally investigated the effect of vibration-assisted drilling on hole oversize and roundness, which are hole quality parameters. Chang and Bone [20] created an analytical model for the estimation of burr height obtained by vibration-assisted and conventional drilling and compared the model with experimental results. Ravisubramanian and Shunmugam [21] experimentally investigated the small thrust force and torque values resulting from micro-hole drilling by measuring them with a high-resolution dynamometer. Experimental research on the impacts of cutting speed and feed rate on thrust force, torque, hole diameter, burr formation, circularity, and roughness was conducted by Uddin *et al* [8]. Chu *et al* [7] experimentally compared the differences between conventional drilling and ultrasonic drilling on material removal amount, torque, and temperature. Moghaddas *et al* [22] experimentally investigated the differences between conventional drilling and ultrasonic drilling in temperature by comparing them according to the parameters of amplitude, feed rate, and cutting speed. Seif *et al* [23] investigated thrust, torque, and temperature by comparing them with numerical, analytical, and combination models. Bain and Raj [24] experimentally investigated the effects of normal drills and the drills they developed for the deep hole drilling process on surface roughness, tool wear, hole oversize, and chip morphology. When the studies in which AA 6061 material is drilled are examined, there are experimental, analytical, and numerical studies, but algorithms such as Taguchi, fuzzy logic, artificial neural networks, and artificial intelligence modeling techniques were not used. Optimization and estimation modeling methods are increasing in popularity day by day, and modeling results are obtained as close as possible to the desired output responses. Different optimization, estimation, and artificial intelligence techniques have been used in studies involving hole drilling. Many problems involving variables with nonlinear and complex interactions are solved using artificial intelligence approaches [18]. From these studies, Dhawan *et al* [25] modeled the thrust force, torque, and delamination factor for drilling fiber-reinforced plastics using ANN, fuzzy logic, and ANFIS. Aguiar *et al* [26] used a multilayer perceptron artificial neural network (MLP ANN), ANFIS,

and a radial basis function (RBF) neural network to estimate the hole diameter for both Ti-6Al-4V and AA2024-T3 materials. Meral *et al* [27] modeled the surface roughness, thrust force and torque obtained by drilling AISI 4140 material with different drill geometries according to Taguchi L16 experimental design by Taguchi analysis and GRA optimization method. Mondal *et al* [28] drilled an aluminum alloy with the Taguchi L27 orthogonal index. In order to optimize the input parameters that will minimize the burr height, they created prediction models with regression analysis and ANN using the Flower Pollination Algorithm. Valarmathi *et al* [29] drilled particleboard composite panels according to Taguchi L27. The response surface method's (RSM) mathematical models and the ANFIS results were compared to the estimation of surface roughness. Kumar and Hynes [30] used ANFIS and a genetic algorithm (GA) for the optimization and estimation of the surface quality of galvanized steels drilled according to the Taguchi L27 orthogonal index. Dedeakayoğulları *et al* [18] used multilayer perceptrons (MLP), learning vector quantization (LVQ), and fuzzy-Mamdani methods for the estimation and optimization of surface roughness in drilling Ti-6Al-4V material. When these methods and studies are examined, it is predicted that Taguchi, ANN, and ANFIS methods can be used to determine the ideal drilling parameters in order to obtain the optimum thrust force, torque, and surface roughness. When the previously used methods are examined, the experimental results are used directly in the classification and analysis of the data. In some cases, the data are normalized to values ranging from 0 to 1, increasing their predictive ability [28]. In the Taguchi method, the mean of the experimental results and the signal-to-noise ratio are used in the analysis and estimation of the output parameters. In some studies in which Taguchi analysis was performed, averages were taken into account in the effect graphs and response tables [15], while in others [31], SN ratios were taken into account. Manoharan *et al* [32] used gray taguchi-based response surface methodology. They used the SN ratios of the experimental results to determine the GRG value and to find the optimum test order. However, a comparison of GRG for experimental results and GRG for SN ratios was not made in this study. The use of SN ratios increases the analysis and prediction abilities of the models. Thus, the predictions made are more in agreement with the experimental results. SN ratios in models made with artificial intelligence techniques were not examined when the literature was reviewed. Clarification of this issue is very important in terms of obtaining effective, accurate, and sensitive results. For this purpose, SN ratios were calculated separately by considering the experimental results of thrust force, torque, and surface roughness output responses. With these calculation results, models were created with Taguchi, ANN, and ANFIS methods for both experimental results and SN ratios. With the help of the created models, prediction results were obtained for each output

response. The performance of the prediction results was compared with parameters such as MAD, MSE, RMSE, and  $R^2$ . With the proposed method, stronger, higher-accuracy models were established, and more accurate predictions were made. Feed rate, cutting speed, and drill length variables were considered input parameters. Optimal input parameters have been determined with response tables and main effects plots in order to obtain optimal output responses in indexable drilling. The effect of drilling AA 6061-T651 material with U drills of different lengths on thrust force, torque, and surface roughness was investigated by comparing the estimation methods and the proposed method. The Taguchi L18 orthogonal index, which is generally preferred as an experimental design method, has been determined [33]. Thus, it was thought that it would be possible to fill a gap in the literature.

## 2. Experimental workflow and method

### 2.1 Workpiece and tools used

6061-T651 aluminum alloy was preferred for the experimental study. Experiment samples were prepared and used in cube sizes of 40 mm. The hole depth is 40 mm. Although the aluminum alloy is certified, the spectra were measured with at least three replications and averaged. Table 1 provides information on the chemical content of the substance based on the spectrum analysis. The average of the hardness measurements of the workpiece was calculated at 115 Brinell. As a result of the mechanical tensile test, the average tensile strength was determined to be 334 MPa, the

yield strength to be 301 MPa, and the elongation value to be 9.5%.

The brand of CNC vertical machining center used in the experiments is the Johnford VMC-850. The operating system is FANUC, and the spindle has a power of 7.5 kW, a top speed of 8000 rpm, with a measuring accuracy of 1  $\mu$ m. An emulsion was prepared by mixing 5% semi-synthetic cutting and cooling fluid with water for the cooling process. Drilling experiments were carried out according to the through-hole and normal hole drilling principles. The cutting tools used in the experiments, the experimental setup, and the measurement method are given in figure 1.

U drills with three different drill lengths were used in the experiments. All U drills have nominal diameters of 20 mm, and drill lengths are different. The ratio of drill length to diameters 3, 4, and 5 was preferred. The dimension information of the U drills used in the experiments is shown in table 2. The dimension information of the cutting inserts used is given in figure 2.

In this study, the central and peripheral inserts of the U drill have different geometric properties, but both are uncoated carbide inserts suitable for aluminum machining. XOET07T205-ND was used as the central insert, and SPET07T208-ND geometry and H01 quality inserts were used for the peripheral insert. U drills of the same nominal diameter and identical inserts were used. At the end of each drilling process, new, unused inserts were attached to the U drill body. A BT-40 VT 25 90 Veldon type tool holder was used to connect the U drill to the spindle. The recommendations from cutting tool catalogs and information from the

**Table 1.** Chemical composition of AA 6061-T651.

Fe	Si	Mn	Cr	Ti	Cu	Mg	Zn	Al
0.5	0.68	0.15	0.17	0.027	0.32	0.98	0.16	Balance

**Table 2.** U drill dimensions used.

U Drills	Diameter (D: mm)	Length (L: mm)
3D	20	60
4D		80
5D		100

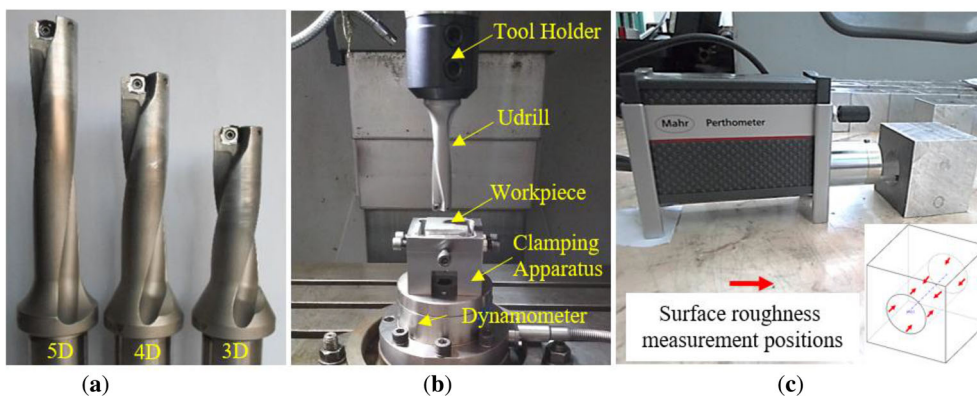


**Figure 1.** (a) U drills used, (b) Experiment setup and (c) Roughness measurement.



Figure 2. Cutting inserts and sizes.

Table 3. Indexable drilling parameters used.

Parameters	Levels		
	1	2	3
Cutting speed, $V_c$ (m/min)	200	250	300
Feed rate, $f$ (mm/rev)	0.06	0.09	–
Drill length/diameter Ratio, LD	3D	4D	5D

literature were taken into consideration when selecting the drilling settings. Table 3 provides the drilling parameters.

The thrust force and torque were measured using a Kistler 9272 dynamometer, and the Kistler 5070A was utilized as an amplifier. In-hole surface roughness measurements of all drilled workpieces were made. For the measurements, the “Mahr Perthometer M1” type surface roughness device in figure 1c was used. The arithmetic average was taken by repeating the measurements from 4 sides, 5 mm inside from both the entrance and the exit of the hole. The arithmetic mean value was determined as the mean surface roughness value ( $R_a$ ). Tracer tip method, scanning speed 0.5 mm/s, cut-off 0.8 mm, scanning length 5.6 mm were determined as a measuring method in the device.

### 2.2 Data preparation

The flow chart of the current study is given in figure 3. In the first stage, a Taguchi L18 orthogonal array was preferred in the experiment design in order to obtain the output parameters according to the input parameters. At the end of the experiments, thrust force and torque data were obtained from the dynamometer. Surface roughness measurements were taken from the roughness measuring device. Using the Minitab 19 program and the least-squares method, the experimental findings of each of the output response were transformed into SN ratios in the second stage. In the third stage, each output response was modeled according to both experimental and SN ratios with Taguchi, ANN, and ANFIS methods. The predictions obtained as a result of the modeling were compared with the experimental results. Minitab 19 software was preferred for Taguchi, and Matlab

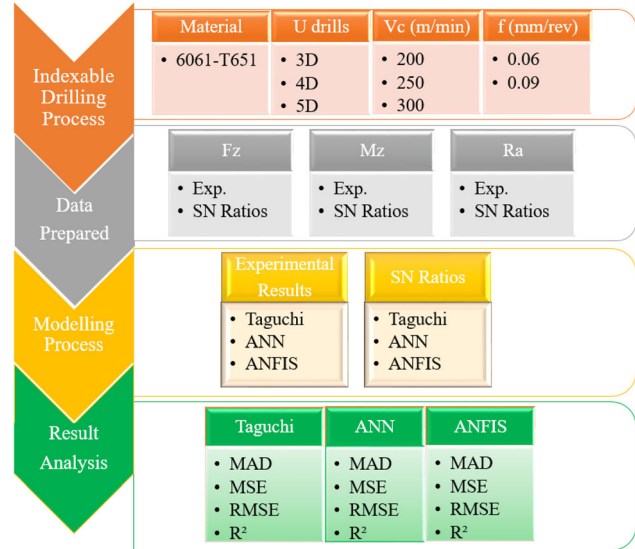


Figure 3. Flow chart.

R2017b software was preferred for ANN, and ANFIS. At the last stage, the estimation results of Taguchi, ANN and ANFIS models created for each output response were calculated and compared according to MAD, MSE, RMSE, and  $R^2$  performance criteria.

### 2.3 Calculation of signal to noise ratios

A number of experimental studies required for modeling and optimization of input parameters with Taguchi can be done with this method. This method provides simultaneous monitoring of controllable and uncontrollable factors by converting the output responses to the logarithmic function signal-to-noise ratio (SN) to determine processing performance. It is used to determine the best input variables for any output response during the manufacturing process. Criteria such as “small is better” and “large is better” are used in calculating SN ratios. As the smaller values of all output responses selected in this study are better, the “small is better” criterion was chosen. Taguchi SN ratios were calculated with the following equation (1).

**Table 4.** Experimental results.

Test No	Drilling parameters			Experimental results			SN ratios of experimental results		
	LD	Vc m/min	f mm/rev	Fz N	Mz Ncm	Ra µm	Fz dB	Mz dB	Ra dB
1	3D	200	0,06	347	333	2,825	− 50.81	− 50.46	− 9.02
2	3D	200	0,09	481	504	5,186	− 53.65	− 54.04	− 14.30
3	3D	250	0,06	433	429	2,983	− 52.74	− 52.64	− 9.49
4	3D	250	0,09	442	443	4,661	− 52.90	− 52.92	− 13.37
5	3D	300	0,06	316	318	2,585	− 49.98	− 50.04	− 8.25
6	3D	300	0,09	466	484	4,150	− 53.37	− 53.69	− 12.36
7	4D	200	0,06	399	369	4,560	− 52.03	− 51.35	− 13.18
8	4D	200	0,09	543	553	9,312	− 54.70	− 54.86	− 19.38
9	4D	250	0,06	334	328	3,733	− 50.47	− 50.33	− 11.44
10	4D	250	0,09	587	606	5,135	− 55.37	− 55.65	− 14.21
11	4D	300	0,06	353	335	3,802	− 50.95	− 50.51	− 11.60
12	4D	300	0,09	431	456	4,829	− 52.70	− 53.17	− 13.68
13	5D	200	0,06	352	344	4,326	− 50.93	− 50.73	− 12.72
14	5D	200	0,09	502	515	3,976	− 54.02	− 54.23	− 11.99
15	5D	250	0,06	358	349	3,654	− 51.07	− 50.85	− 11.25
16	5D	250	0,09	491	503	5,255	− 53.82	− 54.03	− 14.41
17	5D	300	0,06	360	370	5,871	− 51.13	− 51.36	− 15.37
18	5D	300	0,09	474	497	4,875	− 53.51	− 53.93	− 13.76

$$\frac{S}{N} = -10 \log \left( \frac{1}{n} \sum_{i=1}^n y_i^2 \right) \tag{1}$$

*n* represents the number of observations, *y<sub>i</sub>* represents the observed data. Experimental results and SN ratios of output responses are given in table 4.

### 3. Experimental results and discussion

Efficiency is essential for the industry. In order to obtain the desired output responses, the optimum input variables must be determined so that the efficiency can be the highest. Optimal input parameters can only be obtained through modeling and optimization. According to the input parameters, the output responses are compared and analyzed individually or in multiples with various estimation and optimization methods. When these methods are examined, different experimental designs are used. One of the best-known of these methods is the Taguchi experimental design method. Experimental results, or SN ratios, are preferred for optimization and prediction in the Taguchi experimental design method. However, in artificial intelligence techniques such as ANN and ANFIS, experimental data sets are used directly or normalized. The use of normalized data sets leads to estimates that are closer to the experimental results. When the literature was examined, the modeling example with ANN and ANFIS could not be reached after converting the experimental results to SN

ratios. The impact of SN ratios on the modeling output was examined in this study. It was found that the use of SN ratios increased the Taguchi and ANN prediction abilities. Estimates made by Taguchi, the ANN, and the ANFIS models were compared with each other. In this study, cutting speed, feed rate, and the ratio of drill length to diameter were determined as input parameters. As output responses, thrust force, torque, and surface roughness were taken into account. The studies carried out are listed below according to the subject headings.

#### 3.1 Determination of optimum factor levels with Taguchi

For the selected output responses (Fz, Mz, and Ra), the minimum values of experimental results are ideal. The largest of the Taguchi SN ratios represents optimum levels. The results of the experiments performed according to Taguchi’s experimental design were analyzed according to response tables and main effect plots. Means or SN ratios were used to analyze these tables and graphs. The response tables according to the mean and SN ratios of all output responses are shown in tables 5, 6, 7, respectively. From these tables, input factors and optimum levels of factors affecting responses can be determined. When the response tables are examined separately according to the means and SN ratios, the order of importance of the input parameters on the output response is ordered according to the delta value. The determination of which of the control factors is

**Table 5.** Response table of the means and SN ratios for Fz.

Symbol	Means					S/N ratios				
	Level 1	Level 2	Level 3	Delta	Rank	Level 1	Level 2	Level 3	Delta	Rank
Vc	437.5	440.8	<b>399.9</b>	40.9	2	– 52.69	– 52.73	– <b>51.94</b>	0.79	2
f	<b>361.3</b>	490.9		129.5	1	– <b>51.12</b>	– 53.78		2.66	1
LD	<b>414.2</b>	441.2	422.8	27	3	– <b>52.24</b>	– 52.7	– 52.41	0.46	3

Bold Levels of optimum Fz

**Table 6.** Response table of the means and SN ratios for Mz.

Symbol	Means					S/N ratios				
	Level 1	Level 2	Level 3	Delta	Rank	Level 1	Level 2	Level 3	Delta	Rank
Vc	436.4	442.9	<b>409.8</b>	33.1	2	– 52.61	– 52.74	– <b>52.12</b>	0.62	2
f	<b>352.8</b>	506.6		153.8	1	– <b>50.92</b>	– 54.06		3.14	1
LD	<b>418.3</b>	441.3	429.5	22.9	3	– <b>52.3</b>	– 52.64	– 52.52	0.34	3

Bold Levels of optimum Mz

**Table 7.** Response table of the means and SN ratios for Ra.

Symbol	Means					S/N ratios				
	Level 1	Level 2	Level 3	Delta	Rank	Level 1	Level 2	Level 3	Delta	Rank
Vc	5.031	<b>4.237</b>	4.352	0.794	3	– 13.43	– <b>12.36</b>	– 12.5	1.07	3
f	<b>3.815</b>	5.264		1.449	2	– <b>11.37</b>	– 14.16		2.79	1
LD	<b>3.731</b>	5.228	4.659	1.497	1	– <b>11.13</b>	– 13.91	– 13.25	2.78	2

Bold Levels of optimum Ra.

more effective is determined according to the delta value. A higher delta value has a higher impact. For example, the response table for Fz is given in table 5. According to the table, the order of importance for Fz is f, Vc, and LD for both means and SN ratios. The optimum Fz was given by Vc<sub>3</sub>, f<sub>1</sub>, and LD<sub>1</sub>. All output responses increase with increasing f values. The main effect plots of all output responses are shown in figures 4, 5, 6, respectively. The optimal levels of factors for each response are clearly visualized with these main effect graphs. For example, the optimum levels of Fz factors determined from the response table are further confirmed by the main effects plot for the SN ratios of Fz shown in figure 4. When the main effect plots obtained for the mean and SN ratios were examined, the levels of importance of the factors were the same. There is no need to repeat the experiment because the points on the two graphs are at the same level, indicating that the experiments were highly accurate [34].

The main effect plots were obtained according to the response tables. Fz and Mz increased with growing f in figures 4 and 5. The delta value of the f values in response tables 5 and 6 is quite high compared to the others. It is

clear that f is the most influential parameter on Fz and Mz. With the rise of Vc, Fz, and Mz first increased slightly, then decreased significantly. Finer chips were formed because of the rising Vc. On the other hand, thinner chips break more easily, facilitating chip evacuation and thus decreasing the Fz and Mz values. For the LD ratio, the U drills create Fz and Mz values close to each other. The delta value is the smallest and has the least effect. When figure 6 is examined, unlike the other output responses, Ra values were negatively affected by the larger LD ratio. Because the axial deviations increase and the in-hole quality is adversely affected by the extended drill length. According to the response tables, Vc<sub>3</sub>, f<sub>1</sub>, and LD<sub>1</sub> were obtained for optimum Fz and Mz, while Vc<sub>2</sub>, f<sub>1</sub>, and LD<sub>1</sub> were obtained for optimum Ra. Choosing a low LD rate, a low f value, and a higher Vc value in drilling AA 6061-T651 material with U drills resulted in more optimum output values.

Chips obtained from drilling experiments with different U drills are similar to each other as in figure 7. At low cutting speeds and feed rates, the chips are in the form of a continuous ribbon. With the expansion in cutting speed and feed rate, shorter and tighter chips were obtained. As the

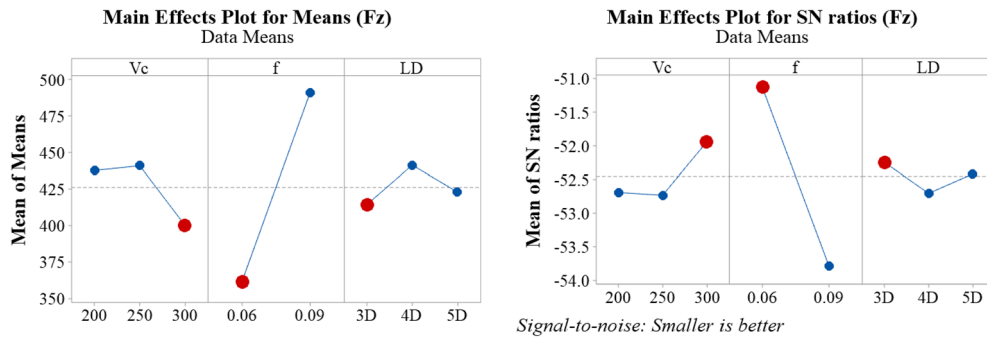


Figure 4. Main effect plots of the means and SN ratios for Fz.

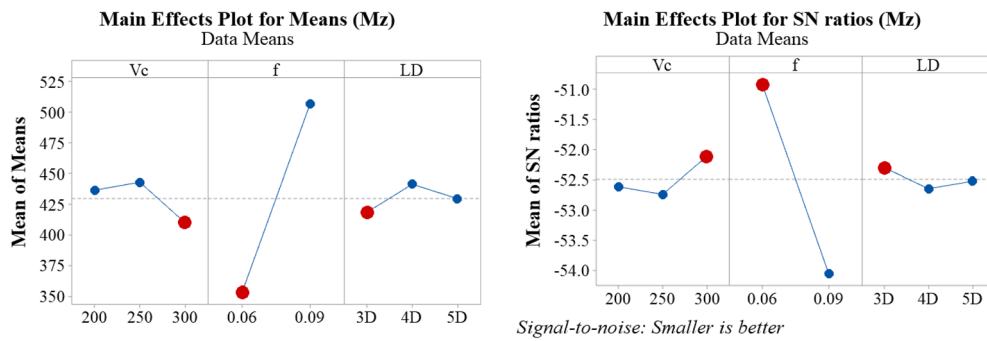


Figure 5. Main effect plots of the means and SN ratios for Mz.

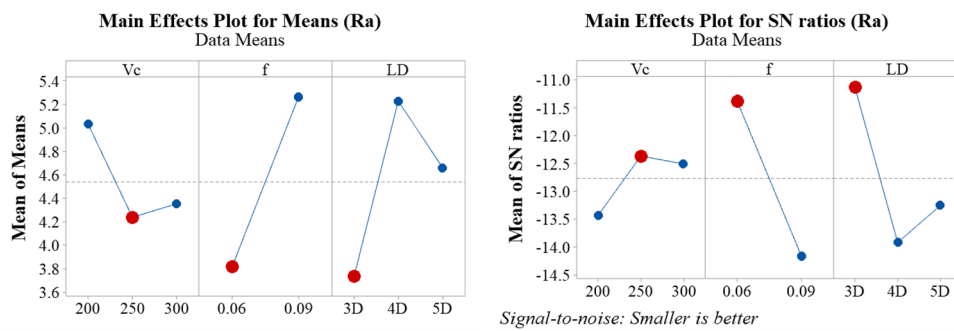


Figure 6. Main effect plots of the means and SN ratios for Ra.

cutting speed and feed rate enlarge, more chips are cut in a shorter time. More chips per unit time cause more power consumption. Thus, the Fz, Mz, and Ra values increase. As the LD ratio of U drills increases, the tendency to increase the through-hole Ra values increases. However, there was no significant difference for Fz and Mz.

It is always desirable to achieve ideal results in optimization and forecasting models. However, when the literature is examined, it is a gap whether the experimental results are used directly or whether the conversion to SN ratios gives more optimal results. This study will reveal which one would be more suitable to obtain more effective models in future studies. For this purpose, by using

Taguchi, ANN, and ANFIS estimation methods, individual output responses were estimated by constructing models according to both experimental results and SN ratios. The performances of the experimental results and the prediction results of the models were compared with methods such as MAPE, MSE, RMSE, and R<sup>2</sup>.

#### 4. Estimation methods

The comparison of experimental results and estimation modeling methods based on SN ratios with each other and the differences between them could not be clarified when

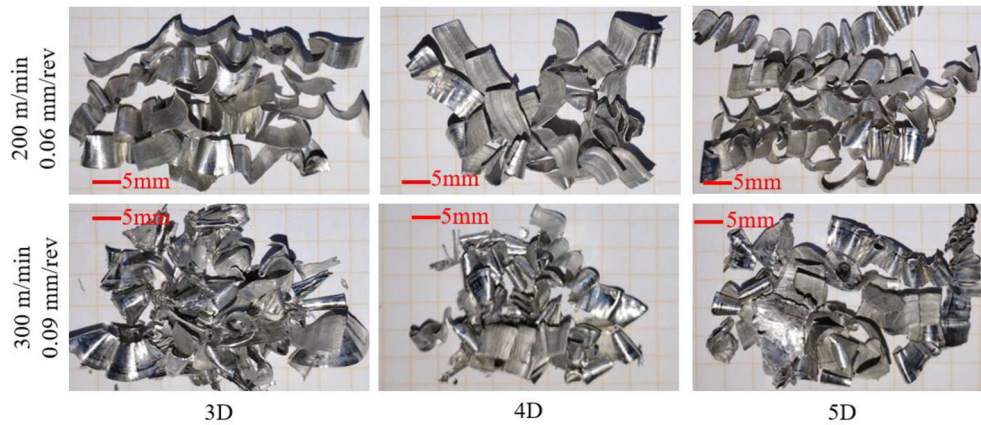


**Figure 7.** Comparison of observed chips.

the literature was examined. In the current study, different estimation methods were examined according to experimental results and SN ratios, and their performances were compared. Using the experimental results and SN ratios, prediction models with Taguchi, ANN, and ANFIS were created for each output response. The experimental results and the predictions obtained from the models were compared. Equation (2) was used to calculate the estimation errors for each output response using the Taguchi, ANN, and ANFIS models. For all output response values, the average percentage error (APE) was calculated using the experimental and predicted values.

$$APE = \left[ \frac{|Exp - Pre|}{Exp} \right] \times 100 \quad (2)$$

*Exp* stands for experimental result and *Pre* stands for predicted result. *APE* is the percent estimation error between the experimental and predicted values.

#### 4.1 Taguchi-based estimation method

SN ratios were determined according to the results of the experiments performed with the Taguchi L18 experimental design. Separate models were obtained for each of the output responses (Fz, Mz, and Ra). Considering these models, all of the experimental results and SN ratios were estimated. “Linear + interactions” were used for both means and SN ratios to obtain Taguchi models. In other words, the terms Vc, f, LD, Vc×f, Vc×LD and f×LD were selected and modeled in the Minitab 19 environment. Estimation values were obtained according to these models. The obtained estimation results and error percentages are given in table 8. According to the findings of the experiment, the mean absolute percentage error (MAPE) was calculated as 5.07%, 5.25%, and 9.07% for Fz, Mz, and Ra, respectively. MAPE, according to the SN ratios, was 0.84%, 0.86%, and 4.55% for Fz, Mz, and Ra, respectively.

Using the experimental results by converting them to SN ratios instead of using them directly in Taguchi prediction models resulted in obtaining values that are more approximate to the output responses of the model. The predictive ability of the model increased significantly, as shown in figure 8. It is clear that the models obtained are sufficient for the estimation of output responses. Using the SN ratio instead of the experimental result reduced MAPE by 83.4% for Fz, 83.6% for Mz, and 49.8% for Ra.

#### 4.2 ANN based estimation method

Artificial neural networks (ANN) are used for modeling output parameters according to input parameters. Some of the data is used for training the model, while other parts are used for testing and estimation. In this study, networks for all output responses are trained using the Levenberg-Marquardt (trainlm) algorithm. The training data set and the test data set were separated from the experimental data set. The test data set did not contain any of the information from the training data set. Five of the data sets were used as the test data set and 13 were selected at random to serve as the training data set. The performance choice was made to be the “mean squared error” (MSE). Experimental results and SN ratios were all subjected to a normalization process ranging from 0 to 1. Normalized values give better results in ANN [35]. Cutting speed, feed rate, and tool length to diameter ratio were determined as input variables. In determining the hidden layers, models were created separately according to one hidden layer (figure 9a) and two hidden layers (figure 9b), and the models with the highest R<sup>2</sup> rating were determined to be the final model. Combinations from 1 to 60 for a single hidden layer and from 1 to 20 for each layer of two hidden layers were examined in order to determine the appropriate model for a single output response. In other words, 60 models were scanned for one hidden layer, and 20 x 20 = 400 models were scanned for



**Table 8.** Experimental and SN ratios error values for Taguchi model.

Test No.	Fz				Mz				Ra			
	Exp.		SN ratios		Exp.		SN ratios		Exp.		SN ratios	
	Pred. N	APE %	Pred. dB	APE %	Pred. Ncm	APE %	Pred. dB	APE %	Pred. μm	Er. %	Pred. dB	APE %
1	359	3	- 51.06	0	350	5	- 50.81	1	2.669	6	- 9.05	0
2	470	2	- 53.40	0	488	3	- 53.70	1	5.342	3	- 14.26	0
3	388	11	- 51.78	2	380	11	- 51.64	2	2.832	5	- 8.98	5
4	487	10	- 53.86	2	492	11	- 53.93	2	4.812	3	- 13.88	4
5	350	11	- 50.68	1	350	10	- 50.70	1	2.892	12	- 8.73	6
6	432	7	- 52.66	1	451	7	- 53.03	1	3.843	7	- 11.88	4
7	385	3	- 51.70	1	354	4	- 50.99	1	5.337	17	- 14.04	7
8	557	3	- 55.02	1	569	3	- 55.21	1	8.535	8	- 18.52	4
9	380	14	- 51.40	2	373	14	- 51.18	2	3.181	15	- 10.75	6
10	541	8	- 54.45	2	561	7	- 54.80	2	5.686	11	- 14.90	5
11	320	9	- 50.35	1	306	9	- 50.01	1	3.577	6	- 11.43	1
12	464	7	- 53.30	1	484	6	- 53.67	1	5.054	5	- 13.85	1
13	354	1	- 51.00	0	343	0	- 50.74	0	3.706	14	- 11.83	7
14	500	0	- 53.95	0	515	0	- 54.22	0	4.596	16	- 12.89	7
15	357	0	- 51.10	0	353	1	- 51.00	0	4.356	19	- 12.46	11
16	492	0	- 53.79	0	499	1	- 53.88	0	4.552	13	- 13.21	8
17	358	0	- 51.02	0	366	1	- 51.19	0	5.789	1	- 15.07	2
18	476	0	- 53.61	0	501	1	- 54.10	0	4.957	2	- 14.07	2
MAPE (%)		5.07		0.84		5.25		0.86		9.07		4.55

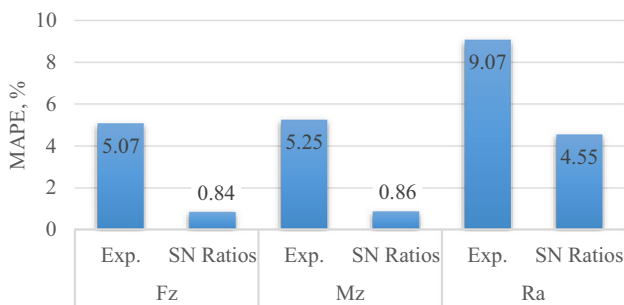


**Figure 8.** MAPE values obtained for Taguchi prediction models.

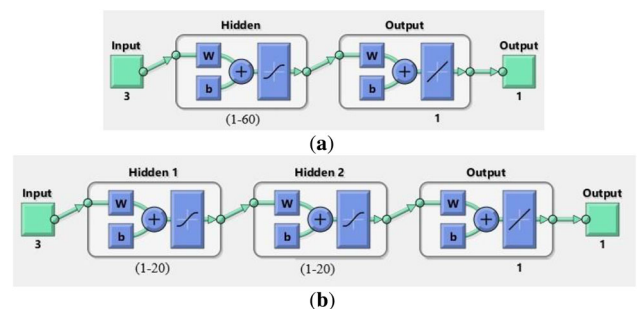


**Figure 9.** (a) Single hidden layer structure and (b) Two hidden layer structure.

two hidden layers. For a total of one output response, a total of 920 models were scanned, with 460 models according to experimental results and 460 models according to SN ratios. The experimental results of the three output responses (Fz, Mz, and Ra) and the SN ratios of  $460 \times 6 = 2760$  models were examined. ANN models are limited to between one and two hidden layers. The experimental results of the three output responses (Fz, Mz, and Ra) and the SN ratios of the  $460 \times 6 = 2760$  models were examined. ANN models are limited to between one and two hidden layers. Because as the number of hidden layers increases, the models become more complex, and the model memorizes the training data (overfitting) [18]. Simpler models perform better in terms of prediction [36]. Only one

**Table 9.** Optimally determined ANN hidden layer numbers.

Fz		Mz		Ra	
Exp.	SN ratios	Exp.	SN ratios	Exp.	SN Ratios
12 - 9	18 - 8	19 - 18	9 - 10	14 - 9	20 - 14

response (Fz, Mz, or Ra) was used as the output layer. Different hidden layers and numbers of neurons were determined for all output responses. The obtained ANN models with optimum accuracy according to the output responses are given in table 9. For all output responses, the results obtained with two hidden layers were found to have

**Table 10.** Experimental and SN ratios error values for ANN model.

Test No.	Fz				Mz				Ra			
	Exp.		SN Ratios		Exp.		SN Ratios		Exp.		SN Ratios	
	Pred. N	APE %	Pred. dB	APE %	Pred. Ncm	APE %	Pred. dB	APE %	Pred. μm	APE %	Pred. dB	APE %
1	347	0	- 50.81	0	334	0	- 50.46	0	2.825	0	- 9.01	0
2	481	0	- 53.86	0	504	0	- 54.05	0	5.186	0	- 14.52	2
3	433	0	- 52.74	0	408	5	- 52.65	0	2.660	11	- 9.52	0
4	442	0	- 52.90	0	443	0	- 53.99	2	4.658	0	- 13.53	1
5	316	0	- 49.98	0	318	0	- 50.04	0	3.088	19	- 8.23	0
6	465	0	- 53.37	0	484	0	- 53.71	0	4.818	16	- 11.50	7
7	400	0	- 52.03	0	370	0	- 51.44	0	4.560	0	- 13.42	2
8	543	0	- 54.70	0	553	0	- 54.85	0	9.311	0	- 19.62	1
9	344	3	- 50.45	0	320	2	- 50.34	0	3.733	0	- 11.49	0
10	587	0	- 55.37	0	607	0	- 55.64	0	5.134	0	- 14.15	0
11	353	0	- 51.53	1	336	0	- 50.51	0	3.802	0	- 12.63	9
12	432	0	- 52.70	0	456	0	- 53.19	0	4.829	0	- 13.97	2
13	352	0	- 51.52	1	344	0	- 50.74	0	4.326	0	- 13.08	3
14	502	0	- 54.02	0	522	1	- 54.55	1	3.976	0	- 11.96	0
15	366	2	- 50.79	1	381	9	- 50.85	0	3.653	0	- 11.27	0
16	471	4	- 53.82	0	502	0	- 54.03	0	5.461	4	- 14.73	2
17	360	0	- 51.13	0	370	0	- 51.36	0	5.871	0	- 15.42	0
18	474	0	- 53.51	0	501	1	- 54.00	0	4.875	0	- 13.58	1
MAPE (%)		0.57		0.18		1.12		1.12		2.80		1.79

higher accuracy. Estimation values and estimation errors obtained according to the created ANN model are given in table 10. According to the experimental results, the mean error (MAPE) was calculated as 0.57%, 1.12%, and 2.8% for Fz, Mz, and Ra, respectively. MAPE, according to the SN ratios, was found to be 0.18%, 0.17%, and 1.79% for Fz, Mz, and Ra, respectively. Using the experimental results by converting them to SN ratios instead of using them directly in ANN prediction models has resulted in values that are closer to the output responses of the model. The predictive ability of the model increased significantly, as shown in figure 10. Using the SN ratio instead of the experimental result reduced MAPE by 68.4% for Fz, 84.8% for Mz, and 36.1% for Ra.

### 4.3 ANFIS based estimation method

Jang [37] first proposed adaptive network-based fuzzy inference systems (ANFIS) in 1993 as an optimization method for elucidating the complicated and nonlinear relationship between input and output variables. It is helpful for calculating complex problems with high levels of uncertainty because it combines the learning capabilities of neural networks with the inference capabilities of fuzzy logic [38]. Sugeno was determined to be the FIS. The ANFIS structure consists of five layers: fuzzification,

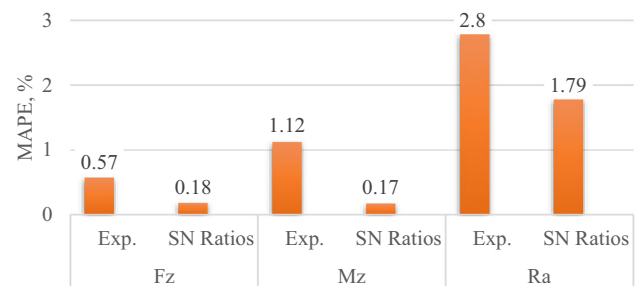


**Figure 10.** MAPE values obtained for ANN prediction models.

product, normalization, defuzzification, and output layer. For the training data set, 70% of the experimental data were chosen at random, and for the test data set, the remaining 30%. 13 of the 18 experiments were found for the training data set and 5 for the test data set in the estimation of each output response. The ANFIS model was created using the MATLAB program’s fuzzy logic toolbox. The model’s input variables included the tool length to diameter ratio, cutting speed, and feed rate. Fz, Mz, and Ra were considered output parameters. The modeled ANFIS structure for a single output response is shown in figure 11. ANFIS performs the optimum estimation for an output response by creating 13 rules in the IF-THEN structure according to the experimental result, or SN ratio.

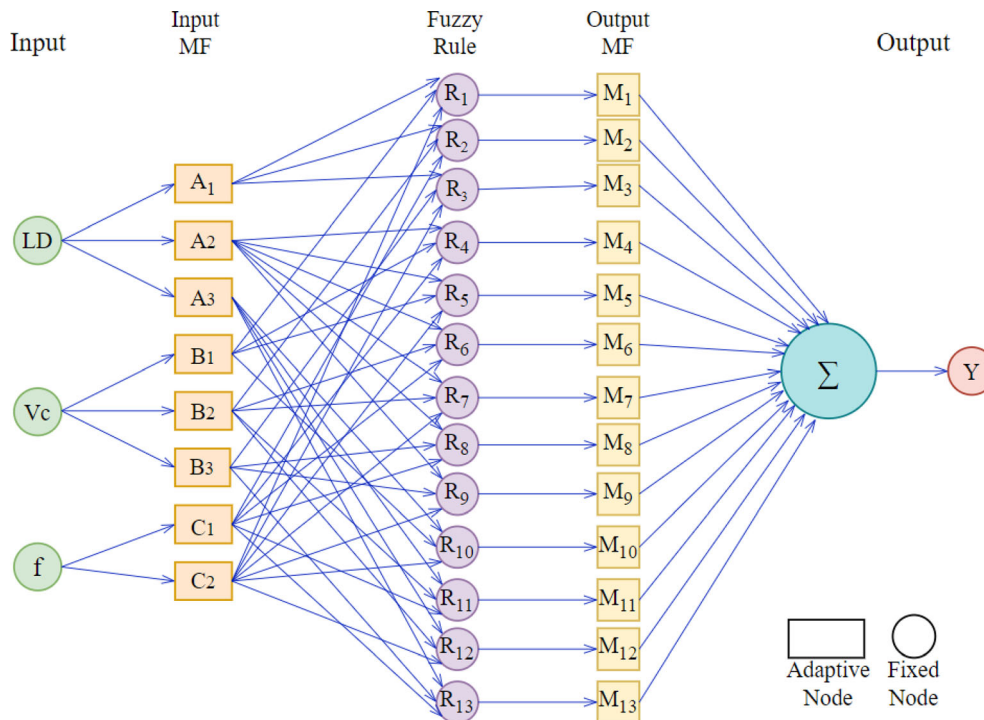


**Figure 11.** Proposed ANFIS architecture.

**Table 11.** Experimental and SN ratios error values for ANFIS model.

Test No.	Fz				Mz				Ra			
	Exp.		SN ratios		Exp.		SN ratios		Exp.		SN ratios	
	Pred. N	APE %	Pred. dB	APE %	Pred. Ncm	APE %	Pred. dB	APE %	Pred. $\mu\text{m}$	APE %	Pred. dB	APE %
1	347	0	- 50.81	0	333	0	- 50.46	0	2.825	0	- 9.02	0
2	481	0	- 48.62	9	504	0	- 54.04	0	5.185	0	- 14.30	0
3	343	21	- 52.74	0	341	21	- 52.65	0	3.614	21	- 9.49	0
4	442	0	- 52.90	0	443	0	- 55.98	6	5.747	23	- 17.75	33
5	316	0	- 49.98	0	318	0	- 56.68	13	3.763	46	- 8.25	0
6	477	2	- 53.37	0	484	0	- 53.69	0	4.828	16	- 13.67	11
7	399	0	- 52.03	0	369	0	- 45.41	12	4.560	0	- 13.18	0
8	487	10	- 54.70	0	553	0	- 54.85	0	9.311	0	- 19.38	0
9	334	0	- 58.64	16	371	13	- 50.33	0	3.733	0	- 11.44	0
10	587	0	- 55.37	0	606	0	- 55.65	0	5.135	0	- 17.87	26
11	353	0	- 50.55	1	335	0	- 50.51	0	3.802	0	- 12.42	7
12	431	0	- 52.70	0	456	0	- 53.17	0	4.829	0	- 13.68	0
13	352	0	- 52.05	2	344	0	- 40.80	20	4.326	0	- 12.72	0
14	502	0	- 54.02	0	477	7	- 49.16	9	3.976	0	- 11.99	0
15	385	8	- 43.01	16	369	6	- 50.85	0	3.653	0	- 11.25	0
16	491	0	- 53.82	0	503	0	- 54.03	0	4.685	11	- 13.23	8
17	353	2	- 51.13	0	370	0	- 51.36	0	5.871	0	- 15.37	0
18	474	0	- 53.51	0	526	6	- 53.93	0	4.874	0	- 13.76	0
MAPE (%)	2.40		2.46		2.90		3.31		6.52		4.69	

The selection of the FIS, epoch number, training data set, and test data set was determined by trial and error. The “sub-clustering FIS system” was used for the efficiency of

the ANFIS model. The epoch was set to 100. Table 11 shows the estimation results, estimation errors, and mean errors of Fz, Mz, and Ra output responses obtained with the

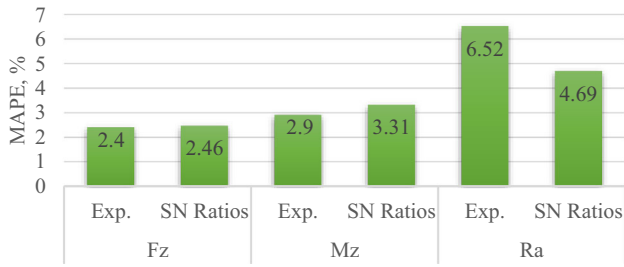


Figure 12. MAPE values obtained for ANFIS prediction models.

Table 12. Accuracy estimation of Taguchi, ANN and ANFIS models.

Models	Fz (N)		Mz (Ncm)		Ra (µm)	
	Exp.	SN ratios	Exp.	SN ratios	Exp.	SN ratios
Taguchi	94.9%	99.2%	94.7%	99.1%	90.9%	95.4%
ANN	99.4%	<b>99.8%</b>	98.9%	<b>99.8%</b>	97.2%	<b>98.2%</b>
ANFIS	97.6%	97.5%	97.1%	96.7%	93.5%	95.3%

Table 13. Comparison of estimation methods for Fz.

Fz Error	Experimental			SN ratios		
	Taguchi	ANN	ANFIS	Taguchi	ANN	ANFIS
MAD	20.922	2.368	10.678	0.440	0.094	1.266
MSE	750.588	31.721	683.455	0.312	0.045	8.801
RMSE	27.397	5.632	26.143	0.558	0.212	2.967
R <sup>2</sup>	0.99599	<b>0.99983</b>	0.99635	0.99989	<b>0.99998</b>	0.9968

ANFIS model. According to the experimental results, MAPE was calculated as 2.4%, 2.9%, and 6.52% for Fz, Mz, and Ra, respectively. MAPE according to SN ratios was found to be 2.46%, 3.31%, and 4.69% for Fz, Mz, and Ra, respectively. The use of experimental results by converting them to SN ratios instead of using them directly in ANFIS prediction models resulted in values closer to the output responses of the Ra model, whereas the opposite situation occurred for Fz and Mz. While the predictive ability of the model increased for Ra, as shown in figure 12, the opposite result was obtained for Fz and Mz. Using the SN ratio instead of the experimental result increased the MAPE by 2.5% for Fz and 14.1% for Mz, while decreasing Ra by 28.1%.

#### 4.4 Comparison of estimation methods

In order to reach the desired thrust force, torque, and surface roughness values in the industry, optimization of the input parameters is required. For this, modeling methods such as Taguchi, ANN, and ANFIS are used. In this study,

Table 14. Comparison of estimation methods for Mz.

Mz Error	Experimental			SN ratios		
	Taguchi	ANN	ANFIS	Taguchi	ANN	ANFIS
MAD	21.695	4.356	12.049	0.450	0.090	1.703
MSE	754.377	90.018	676.969	0.302	0.070	11.843
RMSE	27.466	9.488	26.019	0.550	0.265	3.441
R <sup>2</sup>	0.99607	<b>0.99953</b>	0.99648	0.99989	<b>0.99997</b>	0.99571

Table 15. Comparison of estimation methods for Ra.

Ra Error	Experimental			SN ratios		
	Taguchi	ANN	ANFIS	Taguchi	ANN	ANFIS
MAD	0.397	0.095	0.230	0.573	0.231	0.631
MSE	0.220	0.047	0.208	0.456	0.130	2.023
RMSE	0.469	0.217	0.457	0.675	0.361	1.422
R <sup>2</sup>	0.99029	<b>0.99793</b>	0.99082	0.99731	<b>0.99923</b>	0.98804

cutting speed, feed rate, and length-to-diameter ratio were determined as input parameters. The effects of input parameters on thrust force, torque, and surface roughness were investigated and modeled. Experimental results of output response values and accuracies of the models created according to SN ratios were calculated with equation (3).

$$Accuracy = \frac{1}{n} \sum_{i=1}^n \left[ 1 - \frac{|Exp(i) - Pre(i)|}{Exp(i)} \right] \times 100 \quad (3)$$

The accuracy values of the models created are given in table 12. When the table is studied, it is evident that the models developed in accordance with the ANN and SN ratios have the highest accuracy of all those produced. It can be said that constructing the models by converting the experimental results into SN ratios will result in higher prediction accuracy. The ANN model estimated the data with an accuracy of 99.8% in the prediction of Fz and Mz and 98.2% in the prediction of Ra.

When tables 13, 14, 15 were examined, the MAD, MSE, RMSE, and R<sup>2</sup> values of the performance outputs were calculated. It is evident that the developed models are highly accurate and reliable predictors. Models based on ANN and SN ratios produced the most precise predictions.

$$MAD = \frac{1}{n} \sum_{i=1}^n |Exp(i) - Pre(i)| \quad (4)$$

$$MSE = \frac{1}{n} \sum_{i=1}^n (Exp(i) - Pre(i))^2 \quad (5)$$

$$RMSE = \sqrt{\frac{1}{n} \sum_{i=1}^n [Exp(i) - Pre(i)]^2} \quad (6)$$

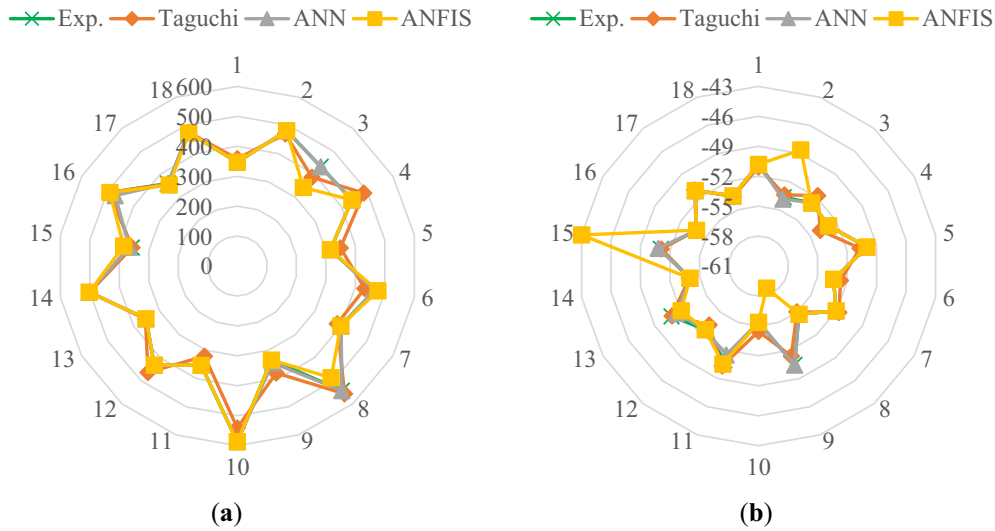


Figure 13. Predictions for Fz. (a) Experimental results and (b) SN ratios.

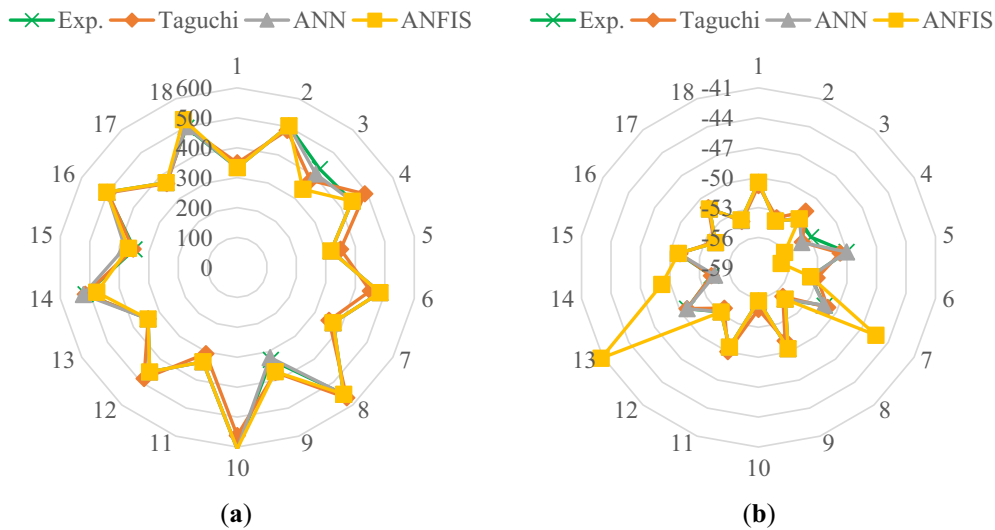


Figure 14. Predictions for Mz. (a) Experimental results and (b) SN ratios.

$$R^2 = 1 - \frac{\sum_{i=1}^n (Exp(i) - Pre(i))^2}{\sum_{i=1}^n (Exp(i) - AverageExp)^2} \quad (7)$$

Here  $n$  is the number of test vector.  $Exp(i)$  is the  $i$  th experimental result.  $Pre(i)$  is the  $i$  th value predicted by the model.  $AverageExp$  is the average of experimental data set.

Experimental results and graphs of SN ratios Taguchi, ANN, ANFIS estimation results can be seen in figure 13 for Fz, figure 14 for Mz, and figure 15 for Ra. When the graphs for Fz are examined, the maximum APE for the models created with the experimental results is 14% with Taguchi, 4% with ANN, and 21% for ANFIS. The maximum APE for models created with SN ratios is 2% with Taguchi, 1% with ANN, and 16% with ANFIS. When the graphs for Mz

are examined, the maximum APE for the models created with the experimental results is 14% with Taguchi, 9% with ANN, and 21% for ANFIS. The maximum APE for models created with SN ratios is 2% with Taguchi, 2% with ANN, and 20% for ANFIS. When the graphs for Ra are examined, the maximum APE for the models created with the experimental results is 19% with Taguchi, 19% with ANN, and 46% for ANFIS. The maximum APE for models created with SN ratios is 11% with Taguchi, 9% with ANN, and 33% with ANFIS. The models constructed with the SN ratios for Fz, Mz, and Ra significantly decreased compared to the maximum APE obtained with the experimental results. However, the reduction in this maximum APE occurred to a lesser extent for ANFIS. The most accurate

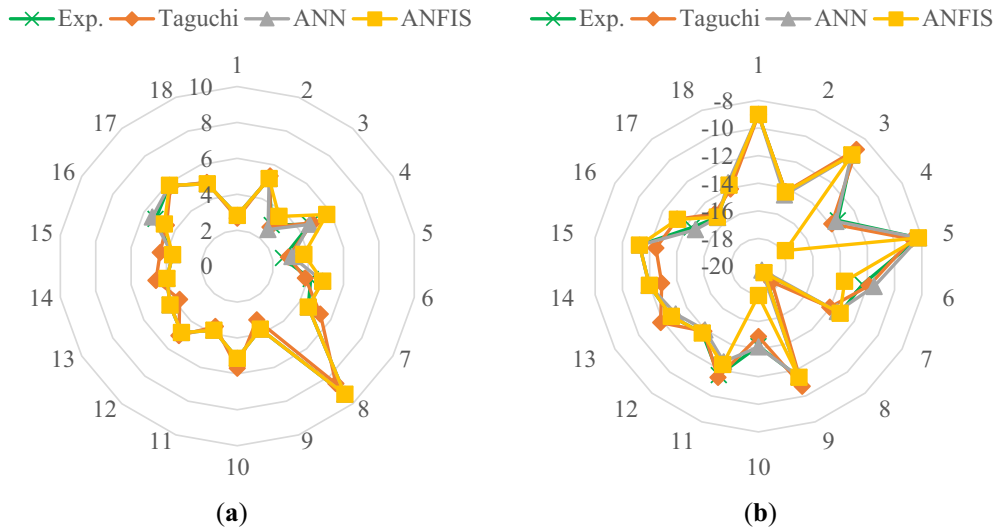


**Figure 15.** Predictions for Ra. (a) Experimental results and (b) SN ratios.

predictions for all output responses were obtained with the ANN model. While the MAD, MSE, RMSE values of the models established with ANN were minimum compared to other estimation methods,  $R^2$  was maximum. This is an indication of the reliability coefficient and predictive ability of ANN models.

## 5. Conclusion

In this study, the effects of feed rate, cutting speed, and length-to-diameter input parameters on the outcomes of thrust force, torque, and surface roughness were investigated. To achieve this, the best input parameters on the output responses were identified by first employing the Taguchi method to analyze the major effect plots and performance replies. Using an experimental data set with Taguchi, ANN, and ANFIS, models were constructed for both experimental results and SN ratios. The predictive ability of the created models was compared with each other. The primary objective of this investigation is to determine which of the prediction models obtained using experimental results and SN ratios contributes to creating models with higher precision. The results obtained with this research are listed below.

- i. According to Taguchi response tables and main effect plots, the  $f$  value was determined as the most effective input parameter on  $F_z$  and  $M_z$ . The optimum input parameters were 300 m/min  $V_c$ , 0.06 mm/rev  $f$ , and 3D U drill for  $F_z$  and  $M_z$ , and 250 m/min  $V_c$ , 0.06 mm/rev  $f$ , and 3D U drill for  $R_a$ .
- ii. When the models created with the Taguchi-based estimation method are compared, using the SN ratio reduced MAPE by 83.4% for  $F_z$ , 83.6% for  $M_z$ , and 49.8% for  $R_a$ .

- iii. When the models created with the ANN-based estimation method are compared, using the SN ratio reduced MAPE by 68.4% for  $F_z$ , 84.8% for  $M_z$ , and 36.1% for  $R_a$ .
- iv. Considering all estimation methods, the models with the highest accuracy were obtained by the ANN estimation method.
- v. When the models created with the ANFIS-based estimation method were compared, using the SN ratio increased MAPE by 2.5% for  $F_z$  and 14.1% for  $M_z$ , while decreasing  $R_a$  by 28.1%.
- vi. For the ANN model created according to the SN ratios, the maximum APE is 1% for  $F_z$ , 2% for  $M_z$ , and 9% for  $R_a$ .
- vii. When the prediction models created were compared, the highest precision values were obtained with the ANN model. These values were calculated as 99.8% for  $F_z$  and  $M_z$ , and 98.2% for  $R_a$ .
- viii. When the  $R^2$  values of the models created according to the experimental results and SN ratios were examined, models with very high reliability were obtained.

## Acknowledgement

This work was supported by the Gazi University Scientific Research Projects Unit with the code 07/2019-08. Authors thank the Gazi University BAP unit for their support.

## Declarations

**Competing interest** The authors declare that they have no known competing financial interests or personal relationships that could have appeared to influence the work reported in this paper.

## References

- [1] Lee W S and Tang Z C 2014 Relationship between mechanical properties and microstructural response of 6061-T6 aluminum alloy impacted at elevated temperatures. *Mater. Des.* 58: 116–124
- [2] Dhakal B and Swaroop S 2020 Effect of laser shock peening on mechanical and microstructural aspects of 6061-T6 aluminum alloy. *J. Mater. Process. Technol.* 282: 116–640
- [3] Rahmati B, Sarhan A A and Sayuti M 2014 Morphology of surface generated by end milling AL 6061-T6 using molybdenum disulfide (MoS<sub>2</sub>) nanolubrication in end milling machining. *J. Clean. Prod.* 66: 685–691
- [4] Rodriguez R I, Jordon J B, Allison P G, Rushing T and Garcia L 2015 Microstructure and mechanical properties of dissimilar friction stir welding of 6061-to-7050 aluminum alloys. *Mater. Des.* 83: 60–65
- [5] Astakhov V P 2014 Drills: science and technology of advanced operations. CRC Press, Boca Raton
- [6] Haitao L, Jia F, Tingke W, Ning C and Huadong L 2021 Numerical simulation and experimental study on the drilling process of 7075-t6 aerospace aluminum alloy. *Materials* 14(3): 553
- [7] Chu N H, Nguyen V D and Do T V 2018 Ultrasonic-assisted cutting: A beneficial application for temperature, torque reduction, and cutting ability improvement in deep drilling of Al-6061. *Appl. Sci.* 8(10): 1708
- [8] Mohammad U, Animesh B, Alokesh P, Sunpreet S, Grzegorz M K and Chander P 2018 Evaluating hole quality in drilling of Al 6061 alloys. *Materials* 11(12): 2443
- [9] Lee B, Liu H and Tarng Y 1998 Modeling and optimization of drilling process. *J. Mater. Process. Technol.* 74(1–3): 149–157
- [10] Parsian A 2018 *Regenerative Chatter Vibration in Indexable Drills: Modeling and Simulation*. PhD Thesis, University West, USA
- [11] Heisel U and Schaal M 2009 Burr formation in short hole drilling with minimum quantity lubrication. *Prod. Eng.* 3(2): 57–163
- [12] Biermann D and Hartmann H 2012 Reduction of burr formation in drilling using cryogenic process cooling. *Procedia CIRP* 3: 85–90
- [13] Kaymakci M, Kilic Z and Altintas Y 2012 Unified cutting force model for turning, boring, drilling and milling operations. *Int. J. Mach. Tools Manuf.* 54: 34–45
- [14] Kilic Z and Altintas Y 2016 Generalized mechanics and dynamics of metal cutting operations for unified simulations. *Int. J. Mach. Tools Manuf.* 104: 1–13
- [15] Rajyalakshmi M and Rao M V 2022 Application of artificial neural networks and genetic algorithm for optimizing process parameters in pocket milling of AA7075. *J. Sci. Ind. Res.* 81: 911–921
- [16] Yalcin U, Karaoglan A D and Korkut I 2013 Optimization of cutting parameters in face milling with neural networks and Taguchi based on cutting force, surface roughness and temperatures. *Int. J. Prod Res.* 51(11): 3404–3414
- [17] Tanikić D 2020 Computationally intelligent optimization of metal cutting regimes. *Measurement* 152: 107358
- [18] Dedeakayoğulları H, Kaçal A and Keser K 2022 Modeling and prediction of surface roughness at the drilling of SLM-Ti6Al4V parts manufactured with pre-hole with optimized ANN and ANFIS. *Measurement* 203: 112029
- [19] Chern G L and Lee H J 2006 Using workpiece vibration cutting for micro-drilling. *Int. J. Adv. Manuf. Technol.* 27(7): 688–692
- [20] Chang S S and Bone G M 2010 Burr height model for vibration assisted drilling of aluminum 6061-T6. *Precis. Eng.* 34(3): 369–375
- [21] Ravisubramanian S and Shunmugam M 2015 On reliable measurement of micro drilling forces and identification of different phases. *Measurement* 73: 335–340
- [22] Moghaddas M, Yi A and Graff K 2019 Temperature measurement in the ultrasonic-assisted drilling process. *Int. J. Adv. Manuf. Technol.* 103(1): 187–199
- [23] Seif C Y, Hage I S and Hamade R F 2019 Utilizing the drill cutting lip to extract Johnson Cook flow stress parameters for Al6061-T6. *CIRP J. Manuf. Sci. Technol.* 26: 26–40
- [24] Bain G and Raj D S 2022 Effect of EDMed rake face grooves on the chip breaking capability of twist drills during deep hole drilling of Al 6061 aluminum alloy. *Mater. Manuf. Process.* 37(9): 1052–1072
- [25] Dhawan V, Debnath K, Singh I and Singh S 2016 A novel intelligent software-based approach to predict forces and delamination during drilling of fiber-reinforced plastics. *Proc. Inst. Mech. Eng. Part L J. Mater. Des. Appl.* 230(2): 603–614
- [26] Aguiar P R, Da Silva R B, Gerônimo T M, Franchin M N and Bianchi E C 2017 Estimating high precision hole diameters of aerospace alloys using artificial intelligence systems: a comparative analysis of different techniques. *J. Brazil. Soc. Mech. Sci. Eng.* 39(1): 127–153
- [27] Meral G, Sarıkaya M, Mıa M, Dilipak H, Şeker U and Gupta M K 2019 Multi-objective optimization of surface roughness, thrust force, and torque produced by novel drill geometries using Taguchi-based GRA. *Int. J. Adv. Manuf. Technol.* 101(5): 1595–1610
- [28] Mondal N, Mandal S and Mandal M C 2020 FPA based optimization of drilling burr using regression analysis and ANN model. *Measurement* 152: 107327
- [29] Valarmathi T N, Palanikumar K, Sekar S and Latha B 2020 Investigation of the effect of process parameters on surface roughness in drilling of particleboard composite panels using adaptive neuro fuzzy inference system. *Mater. Manuf. Process.* 35(4): 469–477
- [30] Kumar R and Hynes N R J 2020 Prediction and optimization of surface roughness in thermal drilling using integrated ANFIS and GA approach. *Eng. Sci. Technol. Int. J.* 23(1): 30–41
- [31] Seçgin Ö and Sogut M Z 2021 Surface roughness optimization in milling operation for aluminum alloy (Al 6061-T6) in aviation manufacturing elements. *Aircraft Eng. Aerosp. Technol.* 93(8): 1367–1374
- [32] Manoharan M, Kulandaivel A, Arunagiri A, Refaai R M A, Yishak S and Buddharsamy G 2021 Statistical modelling to study the implications of coated tools for machining AA 2014 using grey taguchi-based response surface methodology. *Adv. Mater. Sci. Eng.* 2021: 1–20
- [33] Lin Z and Yang C 2010 Combining the Taguchi method with an artificial neural network to construct a prediction model for near-field photolithography experiments. *Proc. Inst.*

- Mech. Eng. Part C J. Mech. Eng. Sci.* 224(10): 2223–2233
- [34] Khorasani A M, Gibson I, Goldberg M and Littlefair G 2018 A comprehensive study on surface quality in 5-axis milling of SLM Ti-6Al-4V spherical components. *Int. J. Adv. Manuf. Technol.* 94(9): 3765–3784
- [35] Tamiloli N, Venkatesan J and SampathKumar T 2022 ANFIS based forecast and parametric investigation during processing activity of AA6082T6. *Mater. Manuf. Process.* 37(1): 99–112
- [36] Pontes F J, Ferreira J R, Silva M B, Paiva A P and Balestrassi P P 2010 Artificial neural networks for machining processes surface roughness modeling. *Int. J. Adv. Manuf. Technol.* 49(9): 879–902
- [37] Jang J S 1993 ANFIS: adaptive-network-based fuzzy inference system. *IEEE Trans. Syst. Man Cybernet.* 23(3): 665–685
- [38] Sharma D, Bhowmick A and Goyal A 2022 Enhancing EDM performance characteristics of Inconel 625 superalloy using response surface methodology and ANFIS integrated approach. *CIRP J. Manuf. Sci. Technol.* 37: 155–173